

CLC\_\_\_\_\_

Number\_\_\_\_\_

UDC\_\_\_\_\_

Available for reference  Yes  No



# Undergraduate Thesis

**Thesis Title:** The Effective Mechanical Properties of  
2-Phase Composite Materials

**Student Name:** Wu Simeng

**Student ID:** 11811324

**Department:** Mechanics and Aerospace Engineering

**Program:** Theoretical and Applied Mechanics

**Thesis Advisor:** Kefu Huang

Date: 10, June, 2022

# **诚信承诺书**

1. 本人郑重承诺所呈交的毕业设计（论文），是在导师的指导下，独立进行研究工作所取得的成果，所有数据、图片资料均真实可靠。
2. 除文中已经注明引用的内容外，本论文不包含任何其他人或集体已经发表或撰写过的作品或成果。对本论文的研究做出重要贡献的个人和集体，均已在文中以明确的方式标明。
3. 本人承诺在毕业设计（论文）选题和研究过程中没有抄袭他人研究成果和伪造相关数据等行为。
4. 在毕业设计（论文）中对侵犯任何方面知识产权的行为，由本人承担相应的法律责任。

作者签名：

2022 年 6 月 10 日

# The Effective Mechanical Properties of 2-Phase Composite Materials

武思蒙

(力学与航空航天工程 系 指导教师：黄克服)

[ABSTRACT]: In this thesis, we derived formulae for effective stiffnesses concerning 2-phase composite materials through a statistical approach. In chapter 2, we introduced motivations and explained the necessity to realize the microstructures in composite materials; In chapter 3, we systematically studied some crucial tools from statistics, with which we then introduced some important functions, in particular, the n-point correlation functions, in an intuitive while rigorous way; In chapter 4, we provided the general method to determine the effective stiffness validated by experiment performed by Baniassadi et al recently.

[Keywords]: microstructures; n-point correlation functions; effective tensor

[摘要]：在本学位论文中，我们用统计方法推导了两相复合材料的等效刚度。第二章介绍在复合材料中引入微结构的动机并阐释其必要性；第三章则系统地研究了一些重要的统计学工具并借此，直观却不失严谨地引入了几个重要的函数，特别地，n 点关联函数；第四章提供了确定等效刚度的一般方法，并采用 Baniassadi 等学者的实验加以验证。

[关键词]：微结构；n 点关联函数；等效张量

# Contents

<b>1. Introduction and scope .....</b>	<b>1</b>
<b>2. An excursion to static microstructure .....</b>	<b>2</b>
2.1 Exhibition of microstructures .....	2
2.2 Why microstructure? .....	6
<b>3. Basic notions .....</b>	<b>8</b>
3.1 Introduction .....	8
3.2 The n-point probability functions .....	10
3.3 Symmetries of correlation functions .....	11
3.4 Ergodicity .....	15
3.5 Case n=2: geometric meaning, asymptotic properties and realizability ...	15
3.6 Other supplementary functions .....	20
3.6.1 Surface correlation functions .....	20
<b>4. The strong-contrast expansions model .....</b>	<b>21</b>
4.1 History of finding a series expansion model .....	21
4.2 Overview of our model .....	21
4.3 Integral relations .....	22
4.4 The effective tensor and the series expansion .....	26
4.5 Experimental validation .....	28
4.5.1 General results .....	28
4.5.2 Experimental procedures .....	29
4.5.3 Numerical implementation .....	29
<b>Conclusions .....</b>	<b>31</b>
<b>Bibliography .....</b>	<b>32</b>

## 1. Introduction and scope

Composite materials are used everywhere in modern technologies, to name a few, nanomechanics, biomechanics and civil engineering. Since every local region of composite materials contains massive information about microstructures, direct computation seems too costly to be realized, that's why people seek for an effective homogeneous medium to replace the origin heterogeneous one.

Poisson was one of the firsts who introduced the notion of effective properties related to magnetism. After then, Mossotti, Clausius followed his method to investigate nonhomogeneous dielectrics. Lorentz published refraction and polarization problems in optics in 1869. Literatures concerning effective mechanical properties are relatively rare in that period. The effective mechanical model was first proposed in 1889 by Voigt. He simply took arithmetic average of elastic moduli of each component to be the effective elastic moduli of the entire composite. The accuracy of arithmetic average is poor as will be shown in section 2.2 where we compare arithmetic average with harmonic average. Reuss added homogeneous deformation field restriction to Voigt's method and the resulting method was known as Voigt-Reuss method. Wiener and Hill showed that Voigt-Reuss method yields good estimates for the upper and lower bounds of effective elastic moduli. The more exact bounds have been proposed by Hashin and Shtrikman by variational method.

The most commonly used three methods dealing with effective properties of heterogeneous materials in recent years are Multiscale Finite Element Method, Asymptotic Homogenization Method with Ansatz and Multipole Expansion Method in Micromechanics of Composites. There are only little literatures exploiting statistical method for the same purpose, which becomes part of the reasons why we choose on the present topic.

In this work, we derive a series expansion of effective elastic moduli in chapter 4. After substituting 1, 2 and 3-point correlation functions, which are defined in chapter 3, into the explicit series, we approximate the effective elastic moduli in contrast to the experimental data. The structure of this thesis is arranged as below: In chapter 2, the least amount of knowledge on microstructures are given, which illuminate the necessity to work on with these microstructures. Chapter 3 investigate general statistical functions as tools to describe the microstructures occurred in chapter 2. With the aid of the previous chapters, we are now able to handle with the effective elastic moduli. Therefore, a strong-contrast

expansion method is developed in chapter 4, served as a general method to determine effective moduli of any 2-phase composite materials. Furthermore, experiments on a certain composite material - the PA-OMMT are conducted to validate the theory proposed in the beginning of the same chapter.

## 2. An excursion to static microstructure

### 2.1 Exhibition of microstructures

Some pictures of microstructure of some typical composites are exhibited.

We make a convention: throughout this chapter 1, 2 and 3, we will constantly abuse the notions of 'heterogeneous media' and 'composite materials' since we can always treat a region as another material, consisting of solid, fluid or air. For example, porous stone is said to be the composite of stone and 'air' (in the voids) in our context. But technically, 2-phase composite and porous media are totally different both mathematically and mechanically. Though, the abuse is sound for statistical approach.

Common **synthetic** example of composite materials:

- aligned and chopped fiber composites

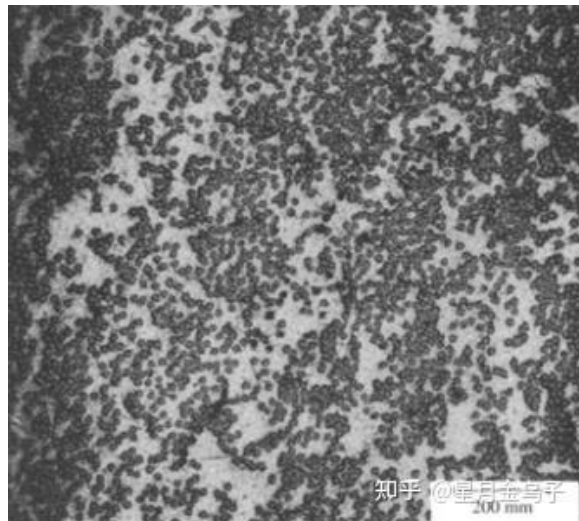


Figure 1.1 光学成像 fiber-reinforced cermet (纤维强化的金属陶瓷, 图为横截面)

- particulate composites

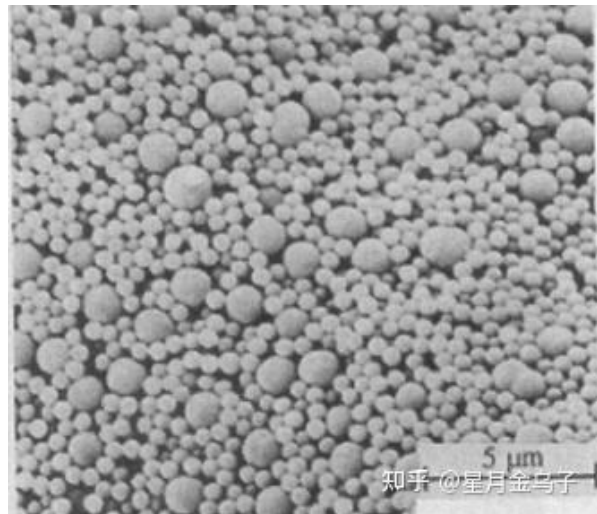


Figure 1.2 扫描电子显微镜下的 colloidal system (由大小各异的微小硬球组成的胶体)

- cellular solids
- gels (This is a particularly hot area recently, but they mostly concern the fabricating process so as to improve the strength of gels, potentially served as smart structure inside organic body)
- foams
- concrete (A famous brittle structure, hardly deform even under tons of normal load, but fails quickly under shear stress. This is why civil engineering use ferroconcrete, concrete composed with rebar - a famous ductile material, stable under shearing force )

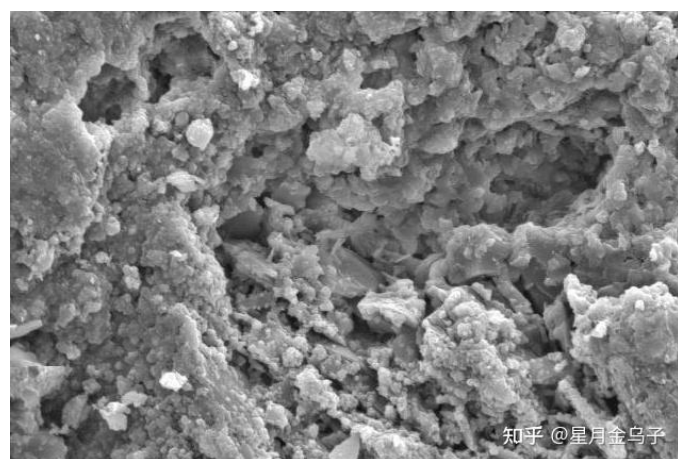


Figure 1.3 显微镜下的混凝土

Common **natural geological** composite materials:

- polycrystals
- soils
- sandstone

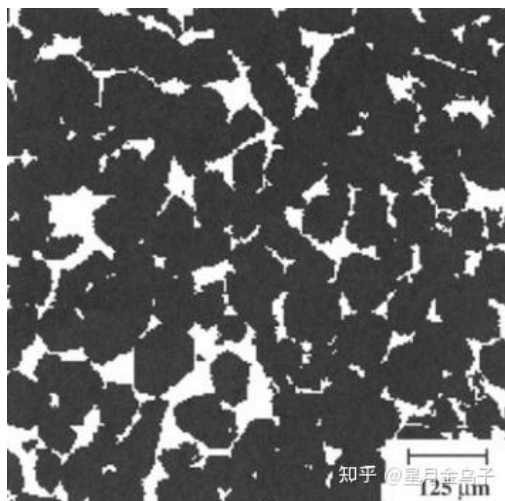


Figure 1.4 一种砂石的 X-ray 显微断层扫描

Surprisingly, the void phase is connected rather isolated via the composite media. Keep in mind that this is a crucial observation! Because then the phase function to be introduced later is defined on open & connected subset of  $\mathbb{R}^d$ , i.e., a region, where functions are defined and upon which calculus are applied.

- Earth's crust
- sea ice
- wood

Some **natural biological** composites:

- bones

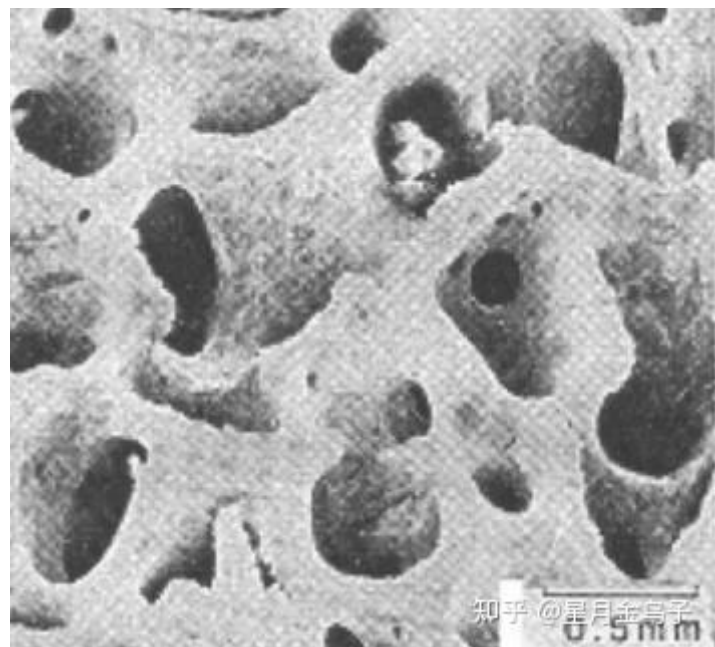


Figure 1.5

- lungs
- blood

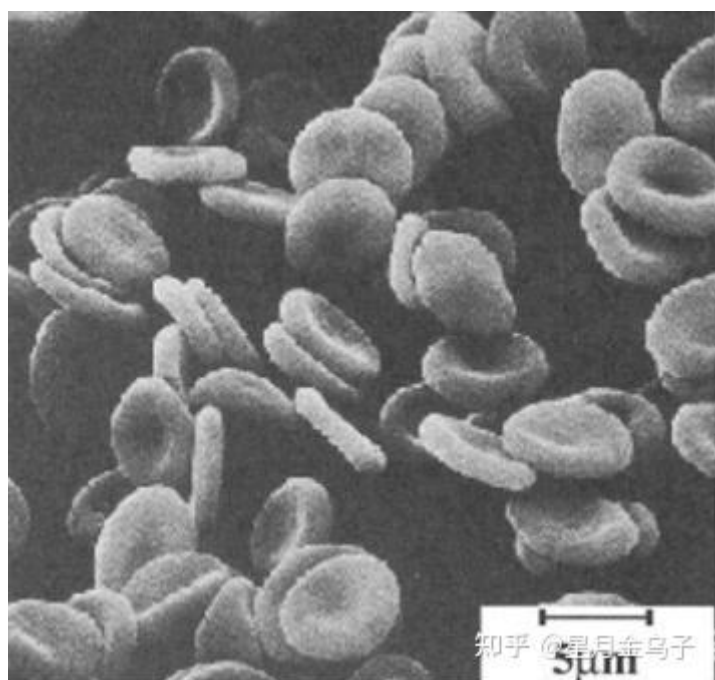


Figure 1.6 红细胞的血液悬浮液

- animal and plant tissue

- cell aggregates and tumors

## 2.2 Why microstructure?

When handling with permeability problems, it seems that the volume fraction (a macroscopic quantity) of pore phase is sufficient to compute the effective permeability coefficient under the assumption that the flow is steady ( $\frac{\partial u}{\partial t} = 0$ ), nonviscous and incompressible. However, flow is just one kind of mass transport phenomenon among various conductivity and transport problem. Generally, the only knowledge is limited for many important problems related to composite materials. Nontrivial features of microstructures are necessary.

The simplest counterexamples are described as follows:

Consider a 2-phase composites. Let  $\phi_1, \phi_2$  denote the volume fractions of these 2 phases respectively. Obviously, one has  $\phi_1 + \phi_2 = 1$ .

We want to compute the effective conductivity of the composites.

Heuristically, we may simply take the arithmetic-average  $\sigma_e = \sigma_1\phi_1 + \sigma_2\phi_2$  to be the effective conductivity. However, this usually grossly overestimates the real  $\sigma_e$ , since this is precisely the effective conductivity of layered composites in the direction along the slabs, as shown figure 7. The more connected the conducting phase is in the composite along slab direction, up to a constant, the larger the effective conductivity can be, usually of the same order of the more conducting phase.

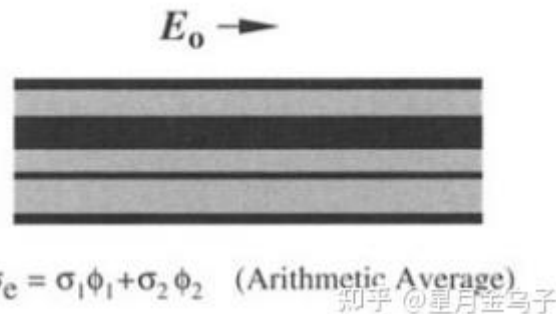


Figure 1.7

On the other hand, one can consider the harmonic average,  $\sigma_e = (\frac{\phi_1}{\sigma_1} + \frac{\phi_2}{\sigma_2})^{-1}$  to be the effective conductivity, correspondingly, this, however, usually underestimates the

effective conductivity since it describes the direction normal to slab as shown in figure 8. Physically if one phase is more insulating, then there'll be little current normal to the slabs.

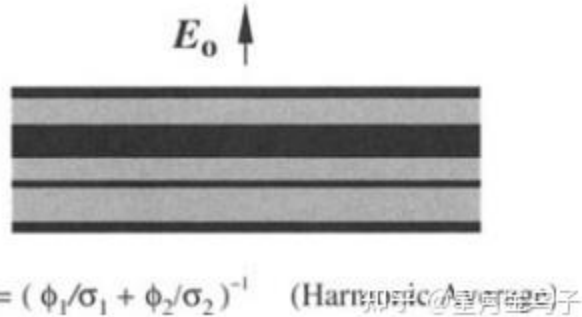


Figure 1.8

In fact, recall the inequality of mean values:

$$H_n \leq G_n \leq A_n \leq Q_n$$

$$\frac{n}{\sum_{i=1}^n \frac{1}{x_i}} \leq \sqrt[n]{\prod_{i=1}^n x_i} \leq \frac{\sum_{i=1}^n x_i}{n} \leq \sqrt{\frac{\sum_{i=1}^n x_i^2}{n}}$$

知乎 @星月金鸟子

we conclude, since two special cases are bounded by the 2 estimates, that:

$$\text{harmonic mean} \leq \text{general } \sigma_e \leq \text{arithmetic mean}$$

Then we claim that we have obtained upper and lower bounds (certainly rough though) of effective coefficients. Further refined estimates are reserved for later discussions.

In a word, this example shows that the ***orientation of microstructure*** is vital for prediction of its conductivity.

Another counterexample occurs when we consider two 50-50 Mixtures, which implies that  $\phi_1 = \phi_2 = 0.5$ , owning the same microstructure but with phases interchanged. However, one phase is connected while the other is not.

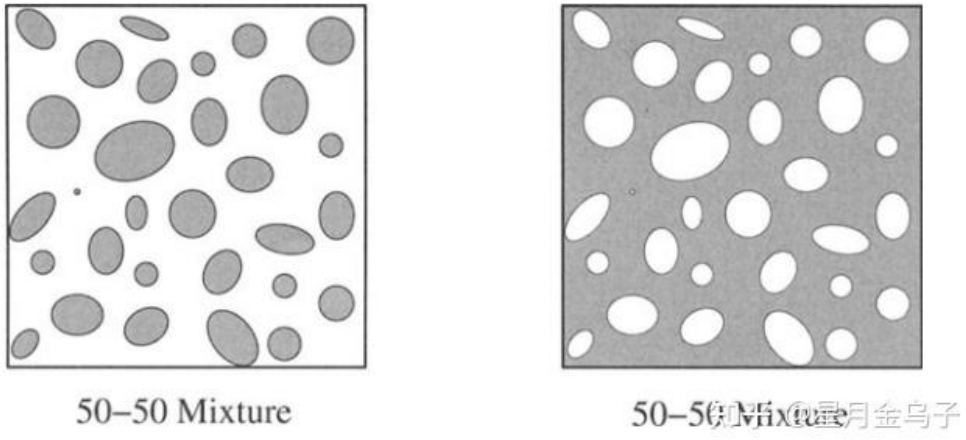


Figure 1.9

Assume the gray phase is significantly stiffer than the white phase. Experiments show that, the right panel in figure 9 generally enjoys higher effective stiffness because the connected phase is stiffer. The outcome is quite intuitive by considering the gray phase as iron and the white phase as glue.

The second counterexample shows that: besides the phase volume fraction and orientation of microstructure, ***connectedness***--a topological property also plays a key role in deciding the effective property of composites.

These 2 simple examples clarified the necessity of study of the microstructures.

### 3. Basic notions

#### 3.1 Introduction

Any sample is a realization of stochastic process. Keep in mind that the phases could be either solid, fluid or void.

**Definition 1.1:** Ensemble is defined to be the collection of all possible realization of a random medium generated by a specific stochastic process.

Let  $(\Omega, \mathcal{F}, \mathcal{P})$  be some fixed probability space, sample space  $\Omega$  represents the outcomes.  $\mathcal{F}$  is  $\sigma$ -ring (closed under countable set operations, i.e.,  $\cap$   $\cup$   $(\cdot)^c$ ) of subsets of  $\Omega$ .  $\mathcal{P}$  is the probability measure assigning a real positive number to each event in  $\Omega$ . Each  $\omega \in \Omega$  corresponds to a realization of the random media  $\mathcal{V} \subset \mathcal{R}^d$ .

Restricting ourselves to two-phase composites, some definitions make sense,

**Definition 1.2:**

- (i) For a given realization  $\omega$ , let  $\mathcal{V}(\omega)$  denotes the whole region occupied by the medium;
- (ii) Given a specific realization  $\omega$ , random phases  $\mathcal{V}_1(\omega)$ ,  $\mathcal{V}_2(\omega)$  are subsets of Euclidean space  $\mathcal{R}^d$  occupied by phase 1 and phase 2 respectively;
- (iii)  $\partial\mathcal{V}(\omega)$  denotes the interface between  $\mathcal{V}_1(\omega)$ ,  $\mathcal{V}_2(\omega)$ .

Observation 1:  $\mathcal{V}_1(\omega) \cup \mathcal{V}_2(\omega) = \mathcal{V}(\omega)$ ,  $\mathcal{V}_1(\omega) \cap \mathcal{V}_2(\omega) = \emptyset$

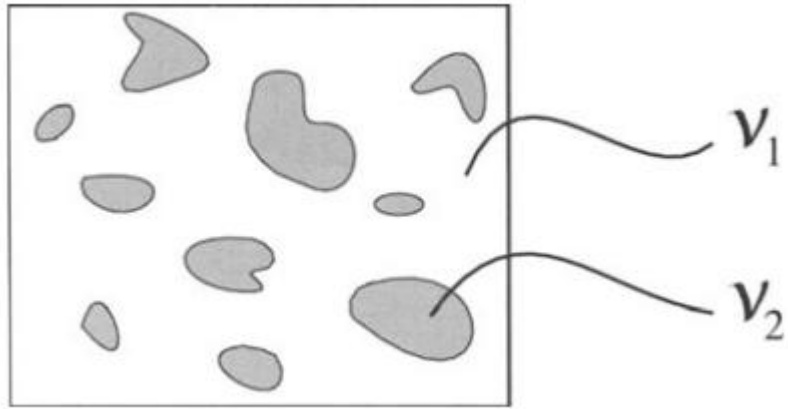


Figure 2.1

Generally, mediums in ensemble are characterized by a random variable  $\xi(x, t; \omega)$ , called **structure function**, which takes different values in different phase but remains the same when  $x$  varying in the same phase. It can be either continuous (e.g., porous sandstone) or discrete (e.g., fiber composites) in spatial variable. Time  $t$  is involved to make evolving problems feasible, however we consider only static microstructure in our scope, so we throw  $t$ -variable from now on, and write  $\xi(x; \omega)$  instead for the structure function.

Definition 1.3:

- (i) Once the realization  $\omega$  is taken on, the structure function degenerates to indicator functions for phase  $i$ ,  $\mathcal{I}^{(i)}(x; \omega) = \begin{cases} 1, & \text{if } x \in \text{phase } i \\ 0, & \text{otherwise} \end{cases} \quad i=1,2.$
- (ii) The indicator function for the interface is defined as

$$\mathcal{M}(x; \omega) \triangleq |\nabla \mathcal{I}^{(1)}(x; \omega)| = |\nabla \mathcal{I}^{(2)}(x; \omega)|$$

Remark: Phase indicator function is precisely the characteristic function in real analysis, but here the term ‘characterization function’ is reserved for later use where it means the Fourier transform of the probability density function. Note that  $\mathcal{I}^{(1)}(x; \omega) + \mathcal{I}^{(2)}(x; \omega) = 1$  since two phases are disjoint with each other; Interface indicator function is a generalized function, the partial derivative here is actually what we

called *distributional derivative* in PDE community. It takes nonzero value only on the interface and is large than  $\infty$ , in fact it is Dirac distribution, which occurs when one tries to differentiate a jump function.

### 3.2 The n-point probability functions

Now fix  $x$ ,  $\mathcal{I}^{(i)}(x)[\omega]$  is a discrete random variable of  $\omega$ , it takes 0 or 1 depending on the specific realization  $\omega$ . The joint frequency function is

$$p(x_i, y_j) = P(X = x_i, Y = y_j).$$

Obviously, we have

$$\mathcal{P}\{\mathcal{I}^{(i)}(x) = 0\} = 1 - \mathcal{P}\{\mathcal{I}^{(i)}(x) = 1\}$$

**Definition 2.1:**  $\langle \cdot \rangle$  is used for *ensemble average*, mathematically, it is the expectation  $E(\cdot)$  of a random variable  $\cdot$ .

Recall the expectation of function of random variables  $E[g(X)]$ . Set  $Y = g(X)$ ,

$$E(Y) = \sum_{x_1, x_2, \dots, x_n} g(x_1, x_2, \dots, x_n) p(x_1, x_2, \dots, x_n)$$

then  $E(Y) = \sum_x g(x)p(x)$  for discrete random variable  $X$ . Similarly, if

$Y = g(X_1, \dots, X_n)$ , we draw our first basic relation

$$\langle f[\mathcal{I}^{(i)}(x)] \rangle = \mathcal{P}\{\mathcal{I}^{(i)}(x) = 1\}f(1) + \mathcal{P}\{\mathcal{I}^{(i)}(x) = 0\}f(0) \quad (2.1)$$

**Definition 2.2:** *One-point probability function* for phase  $i$  is defined as

$$S_1^{(i)}(x) \triangleq \langle \mathcal{I}^{(i)}(x) \rangle = \mathcal{P}\{\mathcal{I}^{(i)}(x) = 1\} \quad (2.2)$$

The second equality follows immediately from letting  $f(x) = x$ . It is also known as *one-point correlation function*.

Physically, it means that if we fix a spacial point  $x$ , and varying in the whole ensemble, the one-point correlation function gives the possibility of finding phase  $i$  at position  $x$ .

Similarly, we can define n-point probability function for phase  $i$  as the expectation of product of indicator functions of phase  $i$

**Definition 2.3:** *n-point probability function* for phase  $i$  is defined as

$$\begin{aligned} S_n^{(i)}(x_1, x_2, \dots, x_n) &\triangleq \langle \mathcal{I}^{(i)}(x_1)\mathcal{I}^{(i)}(x_2) \cdots \mathcal{I}^{(i)}(x_n) \rangle \\ &= \mathcal{P}\{\mathcal{I}^{(i)}(x_1) = 1, \mathcal{I}^{(i)}(x_2) = 1, \dots, \mathcal{I}^{(i)}(x_n) = 1\} \\ &= \text{Probability that } n \text{ points at} \\ &\quad x_1, x_2, \dots, x_n \text{ are found in phase } i \end{aligned} \quad (2.3)$$

To generalize this relation, it amounts to consider

$$\begin{aligned}
& \mathcal{P}\left\{\mathcal{I}^{(i)}(x_1) = j_1, \mathcal{I}^{(i)}(x_2) = j_2, \dots, \mathcal{I}^{(i)}(x_n) = j_n\right\} \\
&= \left\langle \prod_{k \in K} \mathcal{I}^{(i)}(x_k) \prod_{l \in L} [1 - \mathcal{I}^{(i)}(x_l)] \right\rangle
\end{aligned} \tag{2.4}$$

Where  $K = \{k \leq n, j_k = 1\}$ ,  $L = \{l \leq n, j_l = 0\}$  are index sets for points  $x$ . The equality can be obtained since the exterior function  $g(Y_1 Y_2 \cdots Y_n) = Y_1 Y_2 \cdots Y_n$ , each  $Y$  is  $X$  or  $1-X$  depending on the value of indicator function, must be 1, and the 0-terms are cancelled out.

Besides, one can express n-point probability function of phase 2 in terms of those of phase 1, vice versa. To be specific, by (2.3),

$$\begin{aligned}
S_n^{(2)}(x_1, x_2, \dots, x_n) &= \left\langle \prod_{j=1}^n [1 - \mathcal{I}^{(1)}(x_j)] \right\rangle \\
&= 1 - \sum_{j=1}^n S_1^{(1)}(\mathbf{x}_j) + \sum_{j < k}^n S_2^{(1)}(\mathbf{x}_j, \mathbf{x}_k) - \sum_{j < k < l}^n S_3^{(1)}(\mathbf{x}_j, \mathbf{x}_k, \mathbf{x}_l) + \dots + (-1)^n S_n^{(1)}(\mathbf{x}_1, \mathbf{x}_2, \dots, \mathbf{x}_n)
\end{aligned} \tag{2.5}$$

Note the s-th sum in (2.5) has  $C_n^s = \frac{n!}{(n-s)!s!}$  terms with factor  $(-1)^s$ . Moreover, the probability of finding  $n_1$  points in phase1 and  $n_2 = n - n_1$  points in phase2 can be expressed in terms of  $S_1^{(1)}, \dots, S_n^{(1)}$ .

The n-point probability functions introduced here are part of the preparation for the rigorous expression of the effective mechanical properties, say, effective elastic moduli, etc. The determination of these functions for many models are left to two chapters later.

### 3.3 Symmetries of correlation functions

In the worst case, the function  $S_n^{(i)}$  depends on the absolute positions  $x_1, \dots, x_n$ , if so, the medium is said to be statistically inhomogeneous. As depicted in the following pictures.

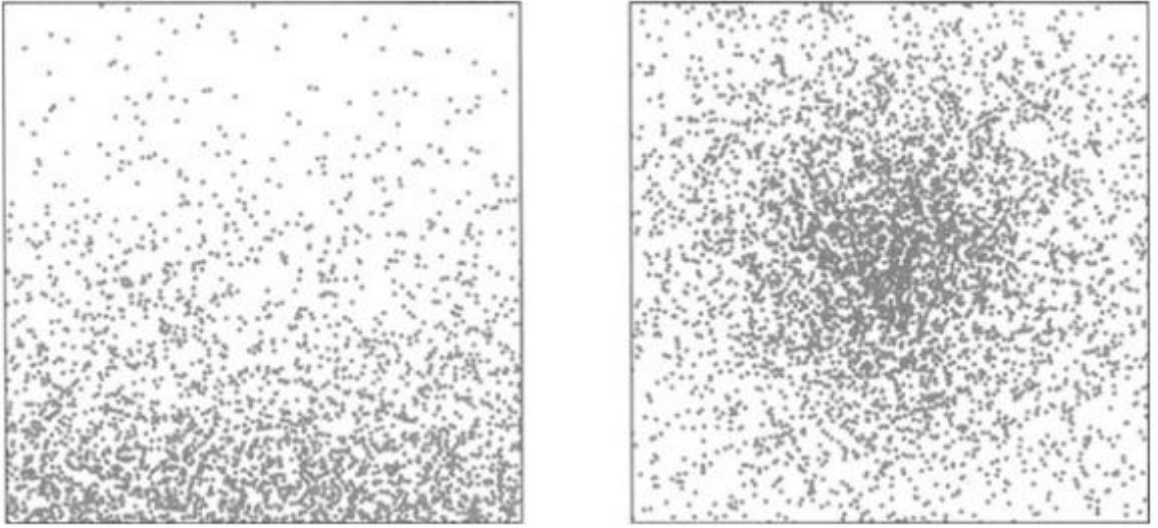


Figure 2.2

Left panel, the density increases downwards; Right panel, density decrease radially from the center

**Definition 2.4:** The medium is said to be (strictly) *statistically homogeneous* if the joint probability distribution functions describing the stochastic process are translational invariant, i.e., the random phase  $\mathcal{V}_i(\omega)$  distinguished by  $\{\mathcal{I}^{(1)}(\mathbf{x}) : \mathbf{x} \in \mathcal{V}\}$  is statistically homogeneous if  $\forall y \in \mathfrak{X}^d$

$$\begin{aligned} & \mathcal{P}\left\{\mathcal{I}^{(i)}(x_1) = j_1, \mathcal{I}^{(i)}(x_2) = j_2, \dots, \mathcal{I}^{(i)}(x_n) = j_n\right\} \\ &= \mathcal{P}\left\{\mathcal{I}^{(i)}(x_1 + y) = j_1, \mathcal{I}^{(i)}(x_2 + y) = j_2, \dots, \mathcal{I}^{(i)}(x_n + y) = j_n\right\} \end{aligned}$$

where n is any positive integer,  $x_1, \dots, x_n$  in  $\mathfrak{X}^d$  and  $j_1, \dots, j_n \in \{0, 1\}$

**Definition 2.5:** The medium is said to be (strictly) *statistically isotropic* if the joint probability distribution functions are rotationally invariant, i.e.,

$$\begin{aligned} & \mathcal{P}\left\{\mathcal{I}^{(i)}(x_1) = j_1, \mathcal{I}^{(i)}(x_2) = j_2, \dots, \mathcal{I}^{(i)}(x_n) = j_n\right\} \\ &= \mathcal{P}\left\{\mathcal{I}^{(i)}(A(x_1 - y) + y) = j_1, \mathcal{I}^{(i)}(A(x_2 - y) + y) = j_2, \dots, \mathcal{I}^{(i)}(A(x_n - y) + y) = j_n\right\} \\ & \quad \forall A \in SO(3) \text{ group} \quad \forall \text{fixed } y \in \mathfrak{X}^3 \end{aligned}$$

Means “Around y, rotate A”

Note: By convention, we say that a medium is statistically isotropic if it's already statistically homogenous.

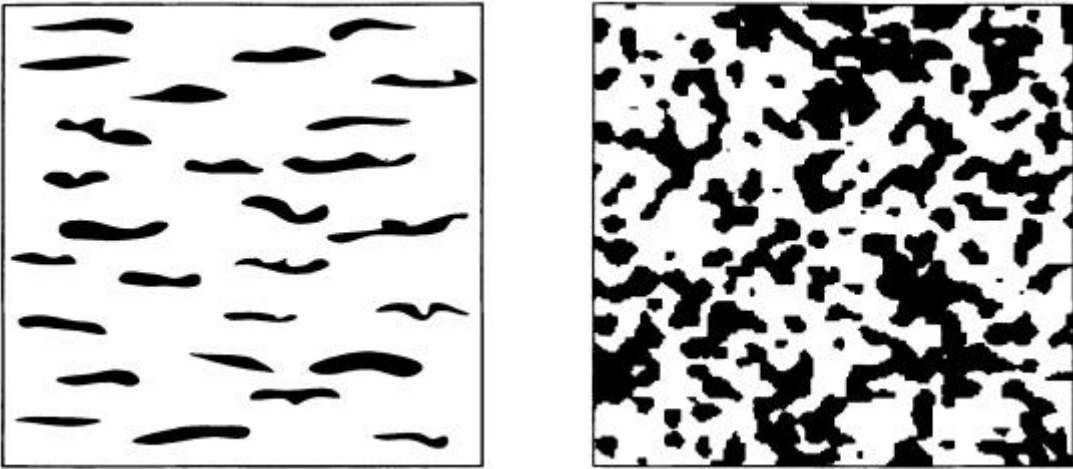


Figure 2.3

Left panel, statistically homogeneous but not that isotropic;

right panel, statistically homogeneous and that isotropic

Remarks:

(i) If the medium is statistically homogeneous, then  $S_n^{(i)}$  depend only on the relative position of  $x_i$ 's. This indicates that we can choose any point as the origin of the medium. In particular, the lowest order function  $S_1^{(i)}$  become constants—the volume fraction  $\phi_i$  of phase i.

Under the same hypothesis, we have a

Claim:

$\mathcal{V}_i(\omega)$  is statistically homogenous if and only if the n-point function

$$S_n^{(i)}(x_1, x_2, \dots, x_n) = S_n^{(i)}(x_1+y, x_2+y, \dots, x_n+y) = S_n^{(i)}(0, x_2-x_1, \dots, x_n-x_1)$$

Proof: Use(2.4)&(2.5).

(ii) If the medium is statistically isotropic,

Claim:

$S_n^{(i)}$  depends only on the distances  $|x_{jk}| = |x_k - x_j|$ ,  $1 \leq j < k \leq n$ .

Proof:  $S_2^{(i)}$ ,  $S_3^{(i)}$  are readily checked. Mathematical induction on index n. Given that

$\mathcal{S}_{n-1}^{(i)}(x_1, x_2, \dots, x_n) \triangleq \langle \mathcal{I}^{(i)}(x_1) \mathcal{I}^{(i)}(x_2) \cdots \mathcal{I}^{(i)}(x_{n-1}) \rangle$  depends only on

$|x_{jk}| = |x_k - x_j|$ . We have  $\mathcal{S}_n^{(i)}(x_1, x_2, \dots, x_n) \triangleq \langle \mathcal{I}^{(i)}(x_1) \mathcal{I}^{(i)}(x_2) \cdots \mathcal{I}^{(i)}(x_n) \rangle$  also depends only on  $|x_{jk}| = |x_k - x_j|$ ?

$$\text{Thus, } \begin{cases} S_2^{(i)}(x_1, x_2) = S_2^{(i)}(x_{12}) \\ S_3^{(i)}(x_1, x_2, x_3) = S_3^{(i)}(x_{12}, x_{13}, x_{23}) \end{cases}$$

The virtue is that  $S_2, S_3$  can be obtained from planar cut, even more,  $S_2$  can be obtained from a linear cut.

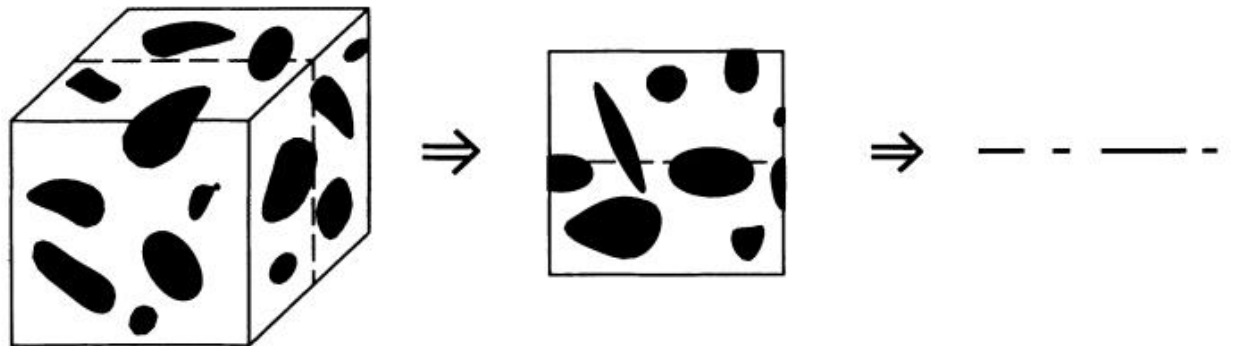
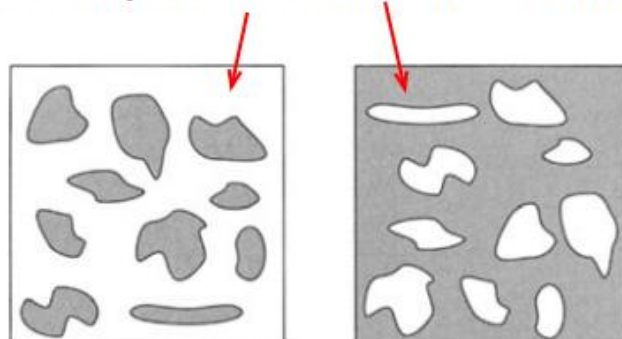


Figure 2.4

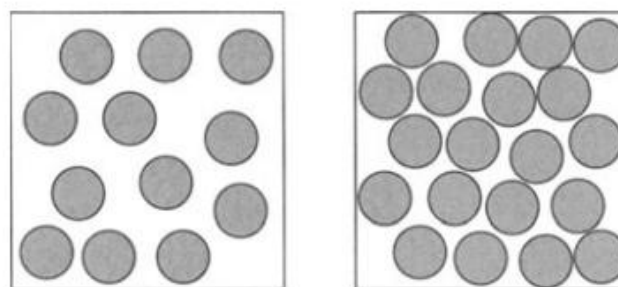
(iii)phase-inversion symmetry

**Definition 2.6:** A random medium is said to possesses phase-inversion symmetry if the morphology of phase 1 at volume fraction  $\phi_1$  is statistically identical to that of phase 2 in the system where the volume fraction of phase 1 is  $1 - \phi_1$ .

statically identical, same volume fraction



Phase-inversion symmetric



Phase-inversion asymmetric

Figure 2.5

Then we draw the following relation

$$S_n^{(1)}(\mathbf{x}^n; \phi_1, \phi_2) = S_n^{(2)}(\mathbf{x}^n; \phi_2, \phi_1) \quad (2.6)$$

At a critical point  $\phi_1 = \phi_2 = 0.5$ , the n-point probability functions for each phase are identical, i.e., geometry of one phase is statistically indistinguishable from the other. This property shows that

**Theorem 2.1:** If the medium is with phase-inversion symmetry at  $\phi_1 = \phi_2 = 0.5$ , then we can express *odd* order point functions in terms of strictly lower order functions.

Explicitly speaking,

$$S_1 = S_2$$

$$2S_{2m+1}^{(2)} = 1 - \sum S_1^{(1)} + \sum S_2^{(1)} - \sum S_3^{(1)} + \dots + (-1)^{2m} \sum S_{2m}^{(1)} \quad (2.7)$$

A common example possessing this symmetry is dispersion of particles.

### 3.4 Ergodicity

The notion of statistically homogeneous roughly speaks that all regions of space are similar as far as statistical properties are concerned. This suggests a famous hypothesis.

*ergodic hypothesis:* The result of averaging over all realizations of the ensemble is equivalent to averaging over the volume for one realization in the infinite-volume limit.

This means that complete probabilistic information can be obtained from a single realization of the infinite medium. We can replace ensemble average by Lebesgue integral of spatial variables.

$$S_n^{(i)}(\mathbf{0}, \mathbf{x}_{12}, \dots, \mathbf{x}_{1n}) = \lim_{V \rightarrow \infty} \frac{1}{V} \int_V I^{(i)}(\mathbf{y}) I^{(i)}(\mathbf{y} + \mathbf{x}_{12}) \dots I^{(i)}(\mathbf{y} + \mathbf{x}_{1n}) d\mathbf{y} \quad (2.8)$$

We refer to such systems as ergodic media.

### 3.5 Case n=2: geometric meaning, asymptotic properties and realizability

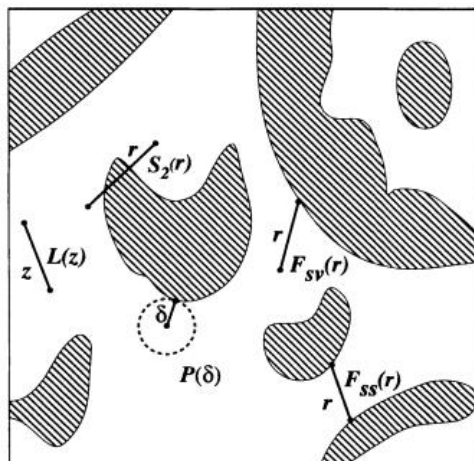


Figure 2.6

For a statistically homogeneous media, the geometric meaning: for a specific orientation, put a needle of length  $r$ , then the probability that both the two ends of the needle are found in phase  $i$  is  $S_2^{(i)}(\mathbf{r})$  as shown above.

Partition a set  $\{\mathbf{x}_1, \mathbf{x}_2, \mathbf{x}_3, \dots, \mathbf{x}_n\}$  into  $L$  subsets  $\{\mathbf{x}_1\}, \{\mathbf{x}_2, \mathbf{x}_3\}, \dots$

Let  $R_{jk}$  denote the distance between centroids of polyhedrons with vertices on points in  $j$ -th,  $k$ -th sets.

**Definition 2.7:** A system is said to possess NO *long-range order* if

$$\begin{aligned} & \lim_{\forall R_{jk} \rightarrow \infty} S_n^{(i)}(\mathbf{x}_1, \dots, \mathbf{x}_n) \\ &= \langle \mathcal{I}^{(i)}(\mathbf{x}_1) \rangle \langle \mathcal{I}^{(i)}(\mathbf{x}_2) \mathcal{I}^{(i)}(\mathbf{x}_3) \rangle \langle \mathcal{I}^{(i)}(\mathbf{x}_4) \mathcal{I}^{(i)}(\mathbf{x}_5) \mathcal{I}^{(i)}(\mathbf{x}_6) \rangle \dots \end{aligned} \quad (2.9)$$

Indeed, relation (2.9) can be extended generally according to the partition of original set, e.g., we can partition  $\{\mathbf{x}_1, \mathbf{x}_2, \mathbf{x}_3, \dots, \mathbf{x}_n\}$  into sets  $\{\gamma\}$ , each with  $m(\gamma)$  elements.

When the media is statistically homogeneous& without long-range order, for  $n=2$ , we have

$$\begin{cases} \lim_{x_{12} \rightarrow 0} S_2^{(i)}(\mathbf{0}, \mathbf{x}_{12}) = \phi_i \\ \lim_{x_{12} \rightarrow \infty} S_2^{(i)}(\mathbf{0}, \mathbf{x}_{12}) = \phi_i^2 \end{cases} \quad (2.10)$$

The first equation in (2.10) holds because in general if  $q+1$  points coincide, say, if  $x_{i_1} = x_{i_2} = \dots = x_{i_{q+1}}$ , then,

$S_n^{(i)}(\mathbf{x}^n) = S_{n-q}^{(i)}(\mathbf{x}_1, \dots, \bar{\mathbf{x}}_{i_1}, \overline{\mathbf{x}_{i_2}, \dots, \mathbf{x}_{i_{q+1}}}, \dots, \mathbf{x}_n)$ , where the bar indicates quantities' absence. Continuity of  $S_2$  follows from the fact that phase  $i$  is an open set, thus if  $\mathbf{0} \in \mathcal{V}^{(i)}$ , a small ball centered at  $\mathbf{0}$  is totally contained in phase  $i$ .

For isotropic media,  $S_2^{(i)}(\mathbf{r})$  attains maximum value of  $\phi_i$  at  $r=0$  and eventually decays (usually exponentially fast) to its asymptotic value of  $\phi_i^2$ .

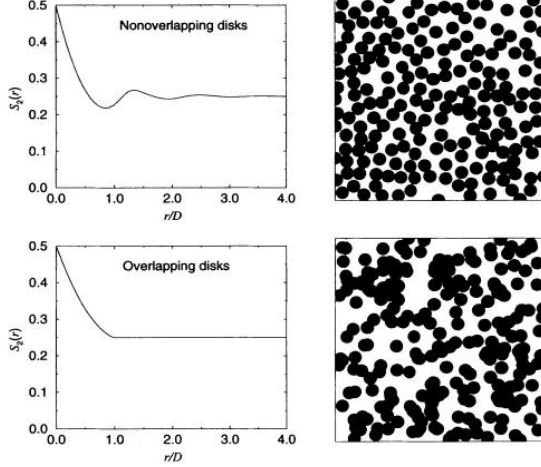


Figure 2.7

**Definition 2.8:** For statistically homogeneous media, the *Autocovariance* of phase 1 is defined as

$$\begin{aligned}\chi(\mathbf{r}) &\triangleq \langle [\mathcal{I}^{(1)}(\mathbf{x}) - \phi_1][\mathcal{I}^{(1)}(\mathbf{x} + \mathbf{r}) - \phi_1] \rangle \\ &= S_2^{(1)}(\mathbf{0}, \mathbf{r}) - \phi_1^2\end{aligned}\quad (2.11)$$

Note that  $\mathcal{I}^{(1)}(\mathbf{x}) - \phi_1$  is a random variable with zero mean, and when in the absence of long-range order, the autocovariance  $\chi(\mathbf{r})$  has the limiting values  $\chi(\mathbf{0}) = \phi_1\phi_2$ ,  $\chi(\infty) = 0$  as a consequence of (2.10). Moreover,  $\chi(\mathbf{r})$  must be semidefinite in the following sense:

$\forall \mathbf{r}_1, \dots, \mathbf{r}_m \in \mathfrak{R}^d$  and arbitrary real numbers  $a_1, \dots, a_m$ ,

$$\sum_{i=1}^m \sum_{j=1}^m a_i a_j \chi(\mathbf{r}_i - \mathbf{r}_j) \geq 0. \quad (2.12)$$

We can then use this to define length scales, for example one length scale arising in fluid permeability (Prager 1961) is defined to be

$$\ell_s = \left\{ \int_0^\infty \mathbf{r} \chi(\mathbf{r}) d\mathbf{r} \right\}^{\frac{1}{2}} = \left\{ \int_0^\infty \mathbf{r} [S_2(\mathbf{r}) - \phi_1^2] d\mathbf{r} \right\}^{\frac{1}{2}} \quad (2.13)$$

**Claim:** autocovariance of phase 1 is **equal** that of phase 2

Proof: Apply (2.5) to statistically homogeneous media.

$$\begin{aligned}1 - (S_1^{(1)}(\mathbf{x}_1) + S_1^{(1)}(\mathbf{x}_2)) + S_2^{(1)}(\mathbf{x}_1, \mathbf{x}_2) &= S_2^{(2)}(\mathbf{x}_1, \mathbf{x}_2), \\ \chi^{(2)}(\mathbf{r}) &= \langle [\mathcal{I}^{(2)}(\mathbf{x}) - \phi_2][\mathcal{I}^{(2)}(\mathbf{x} + \mathbf{r}) - \phi_2] \rangle \\ &= S_2^{(2)}(\mathbf{0}, \mathbf{r}) - \phi_2^2 = S_2^{(2)}(\mathbf{0}, \mathbf{r}) - (1 - \phi_1)^2 \\ &= S_2^{(2)}(\mathbf{0}, \mathbf{r}) - 1 - \phi_1^2 + 2\phi_1 = S_1^{(1)}(\mathbf{0}, \mathbf{r}) - \phi_1^2 = \chi(\mathbf{r})\end{aligned}$$

■

Now we are going to determine the explicit expression of  $S_2$  via scattering of radiation. The normalized scattered intensity  $i(k)$  at wave number  $k$  for 3-dimensional *isotropic* (thus  $S_2$  depends only on a scalar quantity  $r$ ) porous media of volume  $V$  is

$$i(k) = 4\pi V n_0^2 \int_0^\infty \chi(r) r^2 \frac{\sin kr}{kr} dr \quad (2.14)$$

a multiple of Fourier transform of  $\chi(r)$ , here  $n_0$  is the mean density of electrons. To obtain  $\chi(r)$ , apply inverse Fourier transform:

$$\chi(r) = S_2(r) - \phi_1^2 = \frac{1}{2\pi^2 V n_0^2} \int_0^\infty i(k) k^2 \frac{\sin(kr)}{kr} dr \quad (2.15)$$

The accuracy of (2.15) depends on whether the experimentally bandlimited scattering curve  $i(k)$  approximates sufficiently closely entire  $i(k)$ .

Then  $S_2$  can be obtained from (2.15). It is shown (Guinier and Fournet 1955, Debye, Anderson and Brumberger 1957) that for any three-dimensional, *isotropic* two-phase media

$$S_2(r) = \phi_1 - \frac{s}{4}r + O(r^2), \quad r \rightarrow 0 \quad (2.16)$$

$s$  is the *specific surface area*, defined to be *interface area* per unit volume. It is worth noting that the coefficient of linear term is related to  $i(k)$  in limit, i.e.,

$$i(k) \sim \frac{2\pi n_0^2 V s}{k^4}, \quad k \rightarrow \infty \quad (2.17)$$

This provides a measurement technique to determine specific surface area. Berryman (1987) showed that (2.17) applies to anisotropic media as well after angular averaging.

From (2.16), the derivative of  $S_2$  at origin is proportional to  $r$ . Indeed, Debye et al. (1957) showed that:

$$\left. \frac{dS_2^{(i)}}{dr} \right|_{r=0} = -\frac{v_{d-1}}{v_d} s \quad (2.18)$$

$$v_d = \frac{\pi^{d/2}}{\Gamma(1+d/2)} \text{ is volume of } d\text{-dimensional unit ball, } v_0 \equiv 1.$$

For example, we have

$$\left. \frac{dS_2^{(i)}}{dr} \right|_{r=0} = \begin{cases} -s/2, & d = 1 \\ -s/\pi, & d = 2 \\ -s/4, & d = 3 \end{cases} \quad (2.19)$$

Kirste and Porod (1962) examined higher order term in (2.16). But this require *additional information* of the medium (Frisch and Stillinger 1963): special isotropic medium whose interface separating void phase and solid phase could be developed locally

in a canonical power series in the local derivatives of the principal radii of curvature  $R_1$ ,  $R_2$  of the surface. If so, then we have

$$S_2(r) = \phi_1 - \frac{s}{4}r \left\{ 1 - r^2 \left[ \frac{1}{12S} \int K_1 K_2 dA + \frac{1}{32S} \int (K_1 - K_2)^2 dA \right] \right\} + \dots \quad (2.20)$$

$$K_1 = \frac{1}{2R_1},$$

Integrals are taken over the interface,  $S$  is the mean interface area,

$$K_2 = \frac{1}{2R_2}, \quad r < \frac{1}{\max\{K_1, K_2\}}.$$

The first integral in (2.20) is related to topological genus  $p$  of the surface by the Gauss-Bonnet integral formula:

$$4 \int K_1 K_2 dA = 4\pi(1 - p)$$

There's no quadratic term  $r^2$  in (2.20).

**Warning:** (2.20) is valid only for surfaces containing no edges, corners, multiple points or any singular points at which the radii of convergence of the canonical expansion (2.20) of surface shrink to 0.

In the last part of the section, we discuss the existence conditions for a physically realizable correlation or autocovariance function to make our definition in this section reasonable and rigorous.

★**Theorem 2.2:** A necessary and sufficient condition for the existence of  $\chi(r)$  of an autocovariance function  $\chi(\mathbf{r})$  of a general stochastically continuous homogeneous process  $\{Y(\mathbf{x}) : \mathbf{x} \in \mathfrak{R}^d\}$  is that it has the spectral representation (Fourier-Stieltjes representation)

$$\chi(\mathbf{r}) = \frac{1}{(2\pi)^d} \int e^{i\mathbf{k} \cdot \mathbf{r}} dZ(\mathbf{k}), \quad (2.21)$$

where  $Z(\mathbf{k})$  is a nonnegative bounded measure.

If  $\chi(\mathbf{r})$  is absolutely integrable, i.e.,  $\int_{\mathfrak{R}^d} |\chi(\mathbf{r})| d\mathbf{r} < \infty$ , then  $dZ(\mathbf{k}) = \tilde{\chi}(\mathbf{k}) d\mathbf{k}$ ,

spectral function

$$\tilde{\chi}(\mathbf{k}) = \int \chi(\mathbf{r}) e^{i\mathbf{k} \cdot \mathbf{r}} d\mathbf{r} \geq 0, \quad \forall \mathbf{k} \quad (2.22)$$

Finally, under this hypothesis,

$$\chi(\mathbf{r}) = \frac{1}{(2\pi)^d} \int \tilde{\chi}(\mathbf{k}) e^{i\mathbf{k} \cdot \mathbf{r}} d\mathbf{k} \quad (2.23)$$

## 3.6 Other supplementary functions

### 3.6.1 Surface correlation functions

It has been an important notion in trapping and flow problems. Make a convention: phase 1 to be fluid or void phase, phase 2 to be solid phase.

**Definition 2.9:** 1-point surface correlation function is the *specific surface*  $s(\mathbf{x})$  (interface area per unit volume) at point  $\mathbf{x}$ , is defined to be the 1-point function of interface indicator function (see definition 1.3, (ii))

$$s(\mathbf{x}) = \langle \mathcal{M}(\mathbf{x}) \rangle \quad (2.24)$$

Remarks:

1. Different to (2.2),  $s(\mathbf{x})$  cannot be interpreted as a probability, since in an analogue to (2.1), we will arrive at a  $0 \cdot \infty$ ;
2. For a statistically homogeneous medium,  $s(\mathbf{x}) = \text{Const. } s$ .

Naturally, the 2-point surface correlation is defined as following:

**Definition 2.10:**

$$\text{surface-void correlation function} \quad F_{sv}(\mathbf{x}_1, \mathbf{x}_2) = \langle \mathcal{M}(\mathbf{x}_1) \mathcal{I}(\mathbf{x}_2) \rangle,$$

$$\text{surface-surface correlation function} \quad F_{ss}(\mathbf{x}_1, \mathbf{x}_2) = \langle \mathcal{M}(\mathbf{x}_1) \mathcal{M}(\mathbf{x}_2) \rangle$$

with all abbreviated superscripts being <sup>(1)</sup>. See also figure 2.6 attached to the title of section 2.5; Moreover, if the medium is homogeneous, then these surface correlation functions depend only on  $\mathbf{r} = \mathbf{x}_2 - \mathbf{x}_1$ ; if it is isotropic, then they depend only on  $r$ , and can be obtained from any plane cut as a consequence of section 2.3.

If there's no long-range order, then  $F_{sv} \rightarrow \langle \mathcal{M} \rangle \langle \mathcal{I} \rangle$ ,  $F_{ss} \rightarrow \langle \mathcal{M} \rangle^2$  as two point separate with each other farther and farther to infinity, which tend to  $s\phi_1$  and  $s^2$  respectively.

We give the volume fraction  $\phi_1$  a name as *porosity*.

Other functions used in applications are listed as below:

- ◊ *Lineal-Path Function*
- ◊ *Chord-Length Density Function*
- ◊ *Pore-Size Function*
- ◊ *Percolation and Cluster Functions*
- ◊ *Nearest-Neighborhood Functions*
- ◊ *Point\q-Particle Correlation Functions*
- ◊ *Surface\Particle Correlation Function*

They will be introduced once there's a need.

## 4. The strong-contrast expansions model

### 4.1 History of finding a series expansion model

Before 1997, macroscopic anisotropic, in which the variations between phase stiffness tensors are small are studied. Formal solutions to the boundary value problem were developed in the form of perturbation series (Dederichs and Zeller 1973; Gubernatis and Krumhansl 1975; Willis 1981). In particular, for statistically isotropic media, the first few terms of this series were given explicitly in terms of statistical correlation functions (Beran and Molyneux 1966; Milton and Phan-Thien 1982). The method is applicable to arbitrary volume fractions. However, the **prominent drawbacks** of this method have two aspects: On one hand, due to the nature of integral operator, one must carry out renormalization procedure to contend with conditionally convergent integrals; On the other hand, these classical perturbation expansions are only valid for media, in which the moduli of phases are nearly the same.

### 4.2 Overview of our model

In this chapter, we mainly focus on a better expansion method initially arose in the seminal paper [3]. It is then generalized by many following papers in the next 10 years, among which we choose [4] as our final model. There're 3 advantages of Torquato's method: 1. The expansions are not just normal, but the coefficients of the tensor are given explicitly; 2. The expansions converges rapidly for a class of dispersions at arbitrary volume fraction; 3. The method is applicable even in the case where the phase moduli differ significantly. We shall firstly discuss the two famous effective tensors of composite media (in our consideration: macroscopically anisotropic but with **statistically homogeneous** microstructure two-phase composite) obtained by means of exact series expansions. Then we analyze the series to derive the effective tensor. Finally, we close the topic by giving an experimental validation being contrasted with the computer simulation based on the modified method.

### 4.3 Integral relations

Recall some basic equations in linear elasticity. The local stress, strain and displacement field obey the following relations:

$$\text{Hooke's law} \quad \boldsymbol{\tau}(\mathbf{x}) = \mathbf{C}(\mathbf{x}) : \boldsymbol{\epsilon}(\mathbf{x}) \quad (3.0 \text{ a})$$

$$\text{Equilibrium equation} \quad \nabla \cdot \boldsymbol{\tau}(\mathbf{x}) = 0 \quad (3.0 \text{ b})$$

$$\text{Geometrical equation} \quad \boldsymbol{\epsilon}(\mathbf{x}) = \frac{1}{2} \left[ \nabla \mathbf{u} + (\nabla \mathbf{u})^T \right] \quad (3.0 \text{ c})$$

**Definition 3.1:** The 4<sup>th</sup>-order **effective stiffness tensor**  $\mathbf{C}^{(e)}$  of such a material is defined according to the averaged Hooke's law:

$$\langle \boldsymbol{\tau}(\mathbf{x}) \rangle = \mathbf{C}^{(e)} : \langle \boldsymbol{\epsilon}(\mathbf{x}) \rangle \quad (3.1)$$

$\sigma$  and  $\epsilon$  are local 2<sup>nd</sup>-order stress and strain tensors.  $\langle \rangle$  denotes the ensemble average.

Local stiffness tensor is written as

$$\mathbf{C}(\mathbf{x}) = \mathbf{C}_1(\mathbf{x}) + \mathbf{C}_2(\mathbf{x}), \quad (3.2)$$

where stiffness tensor for homogeneous phase  $p=1,2$  is given in terms of **bulk modulus**  $K_p$  and **shear modulus**  $G_p$

$$\mathbf{C}_p = dK_p \boldsymbol{\Lambda}_h + 2G_p \boldsymbol{\Lambda}_s. \quad (3.3)$$

$d$  is the dimension of ambient space and  $\boldsymbol{\Lambda}_h, \boldsymbol{\Lambda}_s$  are 4-th order **hydrostatic** and **shear projection tensors** respectively as exploited in [1]. It can be shown that:

$$(\boldsymbol{\Lambda}_h)_{ijkl} = \frac{1}{d} \delta_{ij} \delta_{kl}, \quad i, j, k, l = 1, 2, \dots, d \quad (3.4)$$

$$(\boldsymbol{\Lambda}_s)_{ijkl} = \frac{1}{2} [\delta_{ik} \delta_{jl} + \delta_{il} \delta_{jk}] - \frac{1}{d} \delta_{ij} \delta_{kl}, \quad i, j, k, l = 1, 2, \dots, d \quad (3.5)$$

Now embed the  $d$ -dimensional ellipsoidal 2-phase composites into an infinite *reference phase* (usual choice is either phase 1 or 2) that is subjected to an applied strain field  $\boldsymbol{\epsilon}_0(\mathbf{x})$

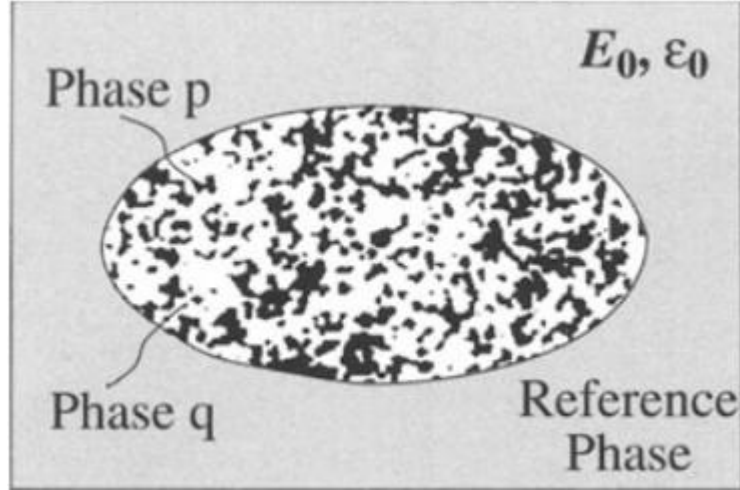


Figure 3.1

**Definition 3.2:** The *induced stress polarization field* is defined to be

$$p(\mathbf{x}) = [\mathbf{C}(\mathbf{x}) - \mathbf{C}_q] : \boldsymbol{\epsilon}(\mathbf{x}) \quad (3.6)$$

It is **symmetric 2<sup>nd</sup>-order tensor**, which **vanishes in phase q** and nonzero in “polarized” phase  $p \neq q$ .

Then by Hooke’s law symmetric stress tensor

$$\boldsymbol{\tau}(\mathbf{x}) = \mathbf{C}_p \boldsymbol{\epsilon}(\mathbf{x}) + p(\mathbf{x}) \quad (3.7)$$

Apply divergence operator on both sides of (3.5), along with the divergence-free property of stress tensor implied by the equilibrium equation without body force, we obtain:

$$(C_q)_{ijkl} \frac{\partial^2 \hat{u}_k(\mathbf{x})}{\partial x_j \partial x_l} = - \frac{\partial p_{ij}(\mathbf{x})}{\partial x_j} \quad (3.8)$$

$$\hat{u}_k(\mathbf{x}) \rightarrow 0, |\mathbf{x}| \rightarrow \infty \quad (3.9)$$

$$\hat{\mathbf{u}}(\mathbf{x}) = \mathbf{u}(\mathbf{x}) - \mathbf{u}_0(\mathbf{x}) \quad (3.10)$$

**Definition 3.3:** The infinite-space Green’s function  $g_{ij}^{(q)}$  is the solution of

$$(C_q)_{ijkl} \frac{\partial^2 g_{im}^{(q)}(\mathbf{x}; \mathbf{x}')}{\partial x_j \partial x_l} = -\delta_{km} \delta(\mathbf{x} - \mathbf{x}') \quad (\text{no summation on q}) \quad (3.11)$$

With

$$g_{km}^{(q)}(\mathbf{x}; \mathbf{x}') \rightarrow 0, |\mathbf{x}| \rightarrow \infty \quad (3.12)$$

Multiplying Green’s function on both sides of (3.6), then conducting integration by parts formula immediately lead to a famous integral relation which has been discovered by many researchers throughout the years in dimension d=3. The **displacement field** is given by:

$$\mathbf{u}(\mathbf{x}) = \mathbf{u}(\mathbf{x}) + \int \{ \nabla g^{(q)}(\mathbf{x}; \mathbf{x}') : p(\mathbf{x}') \} d\mathbf{x}' \quad (3.13)$$

$\mathbf{u}_0$  is displacement field at infinity. Following the comment after Definition 3.2, due to appearance of  $\mathbf{p}(\mathbf{x})$ , the integration region is actually restricted in the ellipsoid.  $\nabla \mathbf{g}$ - the gradient of a tensor is by Gurtin the linear operator from  $\mathfrak{R}^3$  to 2<sup>nd</sup>-order tensor space  $\mathcal{W}$ . So, the integrand is vector-valued function with fixed  $\mathbf{x}$ , integrate with respect to  $\mathbf{x}'$  which is compatible with LHS of (3.11), which is the displacement field  $\mathbf{u}(\mathbf{x})$ .

The solution to d-dimensional Green's function satisfying (3.9) (3.10) is given (Torquato 1997) as below:

$$g_{ij}^{(q)}(\mathbf{r}) = \begin{cases} \frac{1}{2\Omega G_q} \ln\left(\frac{1}{|\mathbf{r}|}\right) \delta_{ij} + b_q n_i n_j, & d = 2 \\ a_q \frac{\delta_{ij}}{|\mathbf{r}|^{d-2}} + b_q \frac{n_i n_j}{|\mathbf{r}|^{d-2}}, & d \geq 3 \end{cases} \quad (3.14)$$

Where  $a_q = \frac{1}{2(d-2)\Omega G_q} \frac{dK_q + (3d-2)G_q}{dK_q + 2(d-1)G_q}$ ,  $b_q = \frac{1}{2\Omega G_q} \frac{dK_q + (d-2)G_q}{dK_q + 2(d-1)G_q}$ ,  $\mathbf{r} = \mathbf{x} - \mathbf{x}'$ ,

$\mathbf{n} = \frac{\mathbf{r}}{|\mathbf{r}|}$ ,  $\Omega = \Omega_d = \frac{2\pi^{\frac{n}{2}}}{\Gamma(\frac{n}{2})}$  is the **surface area of d-dimensional unit ball**, given in [5].

Review on (3.11), since the Green's function has a singularity at  $\mathbf{x}' = \mathbf{x}$ , the integral is actually an **improper integral** that converges when the volume of the excluded integration region containing singularity shrinks to 0.

We seek for strain field from displacement field (3.11), to this end, just differentiate (3.11). However, to overcome the difficulty induced by improper integral, we should first exclude a spherical region centered at  $\mathbf{x}' = \mathbf{x}$ , then take differentiation, and perform integration by parts with a note of divergence theorem, finally let the region tends to 0. The **strain field** is then given (Torquato 1997) by:

$$\boldsymbol{\epsilon}(\mathbf{x}) = \boldsymbol{\epsilon}_0(\mathbf{x}) + \int \mathbf{G}^{(q)}(\mathbf{r}) : \mathbf{p}(\mathbf{x}') d\mathbf{x}' \quad (3.15)$$

With all letters having consistent meaning as in (3.12), and

$$\mathbf{G}^{(q)}(\mathbf{r}) = -\mathbf{D}^{(q)}\delta(\mathbf{r}) + \mathbf{H}^{(q)}(\mathbf{r}) \quad (3.16)$$

Remark: Obviously, constant 4<sup>th</sup>-order tensor  $\mathbf{D}$  associates with Dirac  $\delta$ -function  $\delta(\mathbf{r})$ , it is **induced by the “cavity”** excluded at first step in obtaining strain field.

$$\mathbf{D}^{(q)} = \frac{\boldsymbol{\Lambda}_h}{dK_q + 2(d-1)G_q} + \frac{d(K_q + 2G_q)\boldsymbol{\Lambda}_s}{G_1(d+2)[dK_q + 2(d-1)G_q]} \quad (3.17)$$

$\mathbf{H}^{(q)}(\mathbf{r}) = \nabla \nabla \mathbf{g}^{(q)}(\mathbf{r})$  is the symmetrized tensor, given in explicit form by Torquato [3].

To list useful, albeit a few components,

$$H_{ijkk}^{(q)}(\mathbf{r}) = \frac{d}{\Omega[dK_q + 2(d-1)G_q]} \frac{1}{|\mathbf{r}|^d} (dn_i n_j - \delta_{ij}) \quad (3.18)$$

$$H_{iilk}^{(q)}(\mathbf{r}) = \frac{d}{\Omega[dK_q + 2(d-1)G_q]} \frac{1}{|\mathbf{r}|^d} (dn_k n_l - \delta_{kl}) \quad (3.19)$$

$$H_{iikk}^{(q)}(\mathbf{r}) = H_{ikik}^{(q)}(\mathbf{r}) = 0 \quad (3.20)$$

Note that integrals involving  $\mathbf{H}^{(q)}$  should be convergent in sense of improper integral.

$\mathbf{H}^{(q)}$  owns both **major and minor symmetry**, i.e.,  $H_{ijkl}^{(q)} = H_{jikl}^{(q)} = H_{ijlk}^{(q)} = H_{klij}^{(q)}$ .

Moreover, surface integral of  $\mathbf{H}^{(q)}$  vanishes at any radius  $R > 0$ .

$$\int_{r=R} \mathbf{H}^{(q)}(\mathbf{r}) d\sigma = 0 \quad (3.21)$$

Substitute (3.14) into (3.13), we obtain the integral equation

**Definition 3.4:** *Cavity strain field  $\mathbf{f}(\mathbf{x})$*  is defined to be

$$\mathbf{f}(\mathbf{x}) = \boldsymbol{\epsilon}_0(\mathbf{x}) + \lim_{\epsilon \rightarrow 0} \int_{|\mathbf{x}' - \mathbf{x}| > \epsilon} \mathbf{H}^{(q)}(\mathbf{x} - \mathbf{x}') : \mathbf{p}(\mathbf{x}) d\mathbf{x}' \quad (3.22)$$

Related to strain field by:

$$\mathbf{f}(\mathbf{x}) = \left\{ \mathbf{I} + \mathbf{D}^{(q)} : [\mathbf{C}(\mathbf{x}) - \mathbf{C}_q] \right\} : \boldsymbol{\epsilon}(\mathbf{x}) \quad (3.23)$$

(3.21) has a more intuitive form showing  $\mathbf{f}(\mathbf{x})$  is a modified strain field equal to the usual strain plus a contribution involving constant 4<sup>th</sup>-order tensor  $\mathbf{D}^{(q)}$ . Recall the remark following (3.14),  $\mathbf{D}^{(q)}$  is induced by the cavity near  $\mathbf{x}' = \mathbf{x}$ . This justifies the name in Definition 3.4. Cavity strain field to elasticity is analogous to Lorentz electric field to dielectric theory, from which we borrow the idea.

Combining (3.4) with (3.21) leads to

$$\mathbf{p}(\mathbf{x}) = \mathcal{L}^{(q)}(\mathbf{x}) : \mathbf{f}(\mathbf{x}) \quad (3.24)$$

where

$$\mathcal{L}^{(q)}(\mathbf{x}) = \{\mathbf{C}(\mathbf{x}) - \mathbf{C}_q\} \left\{ \mathbf{I} + \mathbf{D}^{(q)} : [\mathbf{C}(\mathbf{x}) - \mathbf{C}_q] \right\}^{-1} \quad (3.25)$$

Now we describe properties of the 4<sup>th</sup>-order tensor  $\mathcal{L}^{(q)}(\mathbf{x})$ . It owns the same symmetry properties as the stiffness tensor  $\mathbf{C}(\mathbf{x})$ . Moreover, if each phases p's and q are isotropic, then (3.3) holds and we can write the tensor in an even more compact form:

$$\mathcal{L}^{(q)}(\mathbf{x}) = \sum_{p=1,2} \mathbf{L}_p^{(q)} \mathcal{I}^{(p)}(\mathbf{x}) \quad (3.26)$$

Where  $\mathbf{L}^{(q)}$  is a constant tensor and  $\mathcal{I}^{(q)}(\mathbf{x})$  is the indicator function of phase q.

$$\mathbf{L}^{(q)} = \mathbf{L}_p^{(q)} = [dK_q + 2(d-1)G_q] \left[ \kappa_{pq} \boldsymbol{\Lambda}_h + \frac{(d+2)G_q}{d(K_q + 2G_q)} \mu_{pq} \boldsymbol{\Lambda}_s \right] \quad (3.27)$$

$$\kappa_{pq} = \frac{K_p - K_q}{K_p + K_{*q}}, \quad K_{*q} = \frac{2(d-1)}{d} G_q \quad (3.28)$$

$$\mu_{pq} = \frac{G_p - G_q}{G_p + G_{*q}}, G_{*q} = \frac{G_q[d^2K_q + 2(d+1)(d-2)G_q]}{2d(K_q + 2G_q)} \quad (3.29)$$

$\kappa_{pq}, \mu_{pq}$  are called bulk and shear modulus polarizabilities respectively.

#### 4.4 The effective tensor and the series expansion

Now we define the effective elasticity tensor  $\mathbf{C}_e = dK_e\boldsymbol{\Lambda}_h + 2G_e\boldsymbol{\Lambda}_s$  via averaged polarization and averaged cavity strain field.

$$\langle \mathbf{p}(\mathbf{x}) \rangle = \mathbf{L}_e^{(q)} : \langle \mathbf{f}(\mathbf{x}) \rangle \quad (3.30)$$

where

$$\begin{aligned} \mathbf{L}_e^{(q)} &= \{\mathbf{C}_e - \mathbf{C}^{(q)}\} \left\{ \mathbf{I} + \mathbf{D}^{(q)} : [\mathbf{C}_e - \mathbf{C}^{(q)}] \right\}^{(-1)} \\ &= [dK_q + 2(d-1)G_q] \left[ \kappa_{eq}\boldsymbol{\Lambda}_h + \frac{(d+2)G_q}{d(K_q + 2G_q)} \mu_{eq}\boldsymbol{\Lambda}_s \right] \\ \kappa_{eq} &= \frac{K_e - K_q}{K_e + K_{*q}}, \quad \mu_{eq} = \frac{G_e - G_q}{G_e + G_{*q}} \end{aligned} \quad (3.31)$$

(3.30) is localized and is totally equivalent to the averaged Hooke's law that defines the effective tensor as in Definition 3.1, equation (3.1).

Note: keep in mind that all the three tensors  $\mathcal{L}^{(q)}$ ,  $\mathbf{L}_e^{(q)}$  and  $\mathbf{H}^{(q)}$  are associated with the reference phase  $\mathbf{q}$ , we shall omit superscript in subsequent discussion for brevity.

Next, we seek for an explicit expression for the effective moduli. Write (3.22) in schematic operator form, viz.,

$$\mathbf{f} = \boldsymbol{\epsilon}^{(q)} + \mathbf{H}\mathbf{p} \quad (3.32)$$

Multiplying the integral equation from the left by  $\mathcal{L}(\mathbf{x})$  yields

$$\mathbf{p} = \mathcal{L}\boldsymbol{\epsilon}^{(q)} + \mathcal{L}\mathbf{H}\mathbf{p} \quad (3.33)$$

Successive substitution of LHS of (3.33) to RHS of (3.33) leads to

$$\begin{aligned} \mathbf{p} &= \mathcal{L}\boldsymbol{\epsilon}^{(q)} + \mathcal{L}\mathbf{H}\mathcal{L}\boldsymbol{\epsilon}^{(q)} + \mathcal{L}\mathbf{H}\mathcal{L}\mathbf{H}\mathcal{L}\boldsymbol{\epsilon}^{(q)} + \dots \\ &\triangleq \mathbf{T}\boldsymbol{\epsilon}^{(q)} \end{aligned} \quad (3.34)$$

With

$$\mathbf{T} = \mathcal{L}[\mathbf{I} - \mathcal{L}\mathbf{H}]^{-1} \quad (3.35)$$

Taking ensemble average of both sides of (3.36) gives

$$\langle \mathbf{p} \rangle = \langle \mathbf{T} \rangle \boldsymbol{\epsilon}^{(q)} \quad (3.36)$$

or

$$\boldsymbol{\epsilon}^{(q)} = \langle \mathbf{T} \rangle^{-1} \langle \mathbf{p} \rangle \quad (3.37)$$

Average (3.32) and substitute (3.37) yields

$$\langle \mathbf{f} \rangle = (\langle \mathbf{T} \rangle^{-1} + \mathbf{H}) \langle \mathbf{p} \rangle \quad (3.38)$$

Compare (3.30) with (3.38), we obtain for effective tensor  $\mathbf{L}_e$ :

$$\mathbf{L}_e^{-1} = \mathbf{H} + \langle \mathcal{L}(\mathbf{I} - \mathcal{L}\mathbf{H})^{-1} \rangle^{-1} \quad (3.39)$$

Therefore (29) can be arranged and expanded as

$$\langle \mathcal{L} \rangle^2 \mathbf{L}_e^{-1} - \langle \mathcal{L} \rangle = - \left[ \langle \mathcal{L}(\mathcal{L}\mathbf{H}) \rangle - \langle \mathcal{L} \rangle^2 \mathbf{H} \right] - \left[ \langle \mathcal{L}(\mathcal{L}\mathbf{H})^2 \rangle - \frac{\langle \mathcal{L}(\mathcal{L}\mathbf{H}) \rangle^2}{\langle \mathcal{L} \rangle} \right] - \dots \quad (3.40)$$

Finally, we have the following series expansion:

$$\phi_p^2 \mathbf{L}^{(q)} : [\mathbf{L}_e^{(q)}]^{-1} = \phi_p \mathbf{I} - \sum_{n=2}^{\infty} \mathbf{B}_n^{(p)} \quad (3.41)$$

where  $\phi_p$  denotes the volume fraction of phase p,  $\mathbf{I}$  is the 4<sup>th</sup>-order identity matrix, and

$$\mathbf{B}_2^{(p)} = \int_{\epsilon} U^{(q)}(x_1, x_2) [S_2^{(p)}(x_1, x_2) - \phi_p^2] dx_2 \quad (3.42)$$

$$\begin{aligned} \mathbf{B}_n^{(p)} = & (-1)^n \left( \frac{1}{\phi_p} \right)^{n-2} \int dx_2 \dots \int U^{(q)}(x_1, x_2) : U^{(q)}(x_2, x_3) : \dots : \\ & U^{(q)}(x_{n-1}, x_n) \Delta_n^{(p)}(x_1, \dots, x_n) dx_n \quad n \geq 3 \end{aligned} \quad (3.43)$$

$r = x - x'$ ,  $t = \frac{r}{|r|}$  remains the same meaning throughout chapter 3.  $\Delta_n^{(p)}(x_1, \dots, x_n)$  is a position dependent determinant of a matrix consist of N-point correlation functions of phase p. The explicit form of  $\Delta_n^{(p)}(x_1, \dots, x_n)$  in lower point N is given in the next section.

Tensor U reads

$$\begin{aligned} U_{ijkl}^{(q)} &= L_{ijmn}^{(q)} H_{mnkl}^{(q)}(r) \\ &= [dK_q + 2(d-1)G_q] \{ [K_{pq} - \frac{(d+2)G_q}{d(K_q + 2G_q)} \mu_{pq}] \frac{\delta_{ij}}{d} H_{mmkl}^{(q)}(r) \\ &\quad + \frac{(d+2)G_q}{d(K_q + 2G_q)} \mu_{pq} H_{ijkl}^{(q)}(r) \} \end{aligned} \quad (3.44)$$

with  $\mu_{pq}$  given in (3.29),  $L^{(q)}$  given in (3.27).

(3.41) is precisely the famous strong-contrast expansion. In a technical view, (3.41) seems obscure since LHS is too abstract, thus it is cumbersome to calculate it out. However, if the composite material owns some symmetries as mentioned in section 2.3, say, if it is statistically isotropic, then the LHS can be enormously simplified! We shall see this in the following section 3.5.

We shall make a brief review on the fluctuation phenomenon to finish the current section.

Taking quadruple dot product of (3.40) with  $\Lambda_h$  and  $\Lambda_s$  respectively, one derives equations for statistically isotropic composite:

$$\frac{K_e + K_{*q}}{K_e - K_q} \left( \sum_{\alpha=1}^2 v_\alpha \kappa_{\alpha q} \right)^2 - \sum_{\alpha=1}^2 v_\alpha \kappa_{\alpha q} = \mathcal{A}_K(K_q, G_q, K_1, G_1, K_2, G_2, \text{microstructure})$$

$$\frac{G_e + G_{*q}}{G_e - G_q} \left( \sum_{\alpha=1}^2 v_\alpha \mu_{\alpha q} \right)^2 - \sum_{\alpha=1}^2 v_\alpha \mu_{\alpha q} = \mathcal{A}_G(K_q, G_q, K_1, G_1, K_2, G_2, \text{microstructure}) \quad (3.45)$$

“microstructure” in round brackets refers to corresponding n-point correlation functions.

Here's an interpretation. The left-hand side of (3.41) is the principal reference term of the strong-contrast expansion, while the right-hand side is the fluctuation term relative to the reference medium with moduli  $K_q$ ,  $G_q$ .

## 4.5 Experimental validation

### 4.5.1 General results

This section provides an experimental result along with numerical analysis to validate our previous model introduced in chapter 3. The result is drawn heavily from Baniassadi's work [7], [8]. The ultimate result is shown intuitively in figure 3.1. Besides, it is also shown in figure 3.2 that the statistical approach stands for a better report of determining effective stiffness in contrast to Mori-Tanaka method.

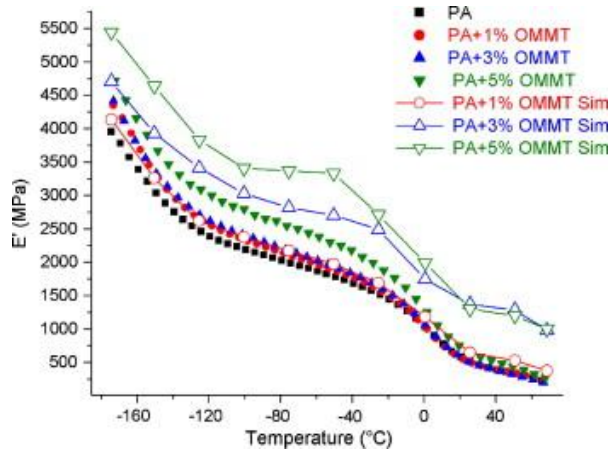


Figure 3.1. Comparison between experimental results and simulation results, first occurred in [8]

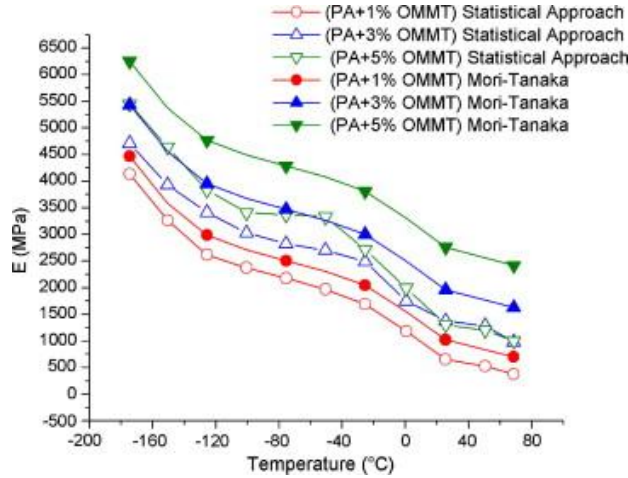


Figure 3.2. Comparison between statistical results and Mori-Tanaka results, in [8]

#### 4.5.2 Experimental procedures

Preparing materials: Baniassadi [7] chose polyamide (PA) resin to be the matrix, chose commercial organo-modified montmorillonite (OMMT) to be the filler. The detailed information concerning the densities, temperatures and concentration of the mentioned materials are given in [7].

Producing composites: Dried PA and OMMT at 80°C for 4h. Then melt and mixing them completely. Put the composite into a co-rotating twin-screw extruder at 180°C at 150 rpm rotation speed for 5 min. The consequent products are PA-OMMT nanocomposite at different weight fraction 0,1,3 and 5 wt.%.

Evaluating mechanical properties: [7] have used Dynamic Mechanical Analyzer (DMA 242C-Netzsch). Storage ( $E'$ ) and loss ( $E''$ ) modulus were measured and recorded as a function of temperature (-175 °C to +70 °C) with a dynamic temperature ramp sweep at 2 K min<sup>-1</sup>. Measurements were performed using the single cantilever bending mode at a frequency of 1 Hz. All DMA sample were hot-pressed and cut in the form of 9.70–10.40 mm-long, 1.15–1.47 mm-thick and 4.95–5.9 mm-wide specimens. To check the reproducibility of the experimental data and to ensure their consistency, three specimens were tested for each formulation.

The experiment's results are shown in figure 3.1 with solid signals.

#### 4.5.3 Numerical implementation

Baniassadi [7] took the isotropic samples with randomly oriented disks to simulate the composites by the soft-core approach.

Since the 1-point correlation function is just the volume fraction of PA in the PA-OMMT nanocomposite as indicated in section 2.2 and 2.3, it can be directly calculated under 0,1,3 and 5 wt.% since the densities of PA and OMMT are known.

Based on the generated model, in the same spirit with Buffon's experiment, Baniassadi [8] obtained the 2-point correlation functions by assigning a large number of random vectors within the generated microstructure and counting the fraction of the vectors that satisfied the condition discussed in section 2.5, due to the geometric meaning of 2-point correlation functions. Figure 3.3 below exhibits the consequences.

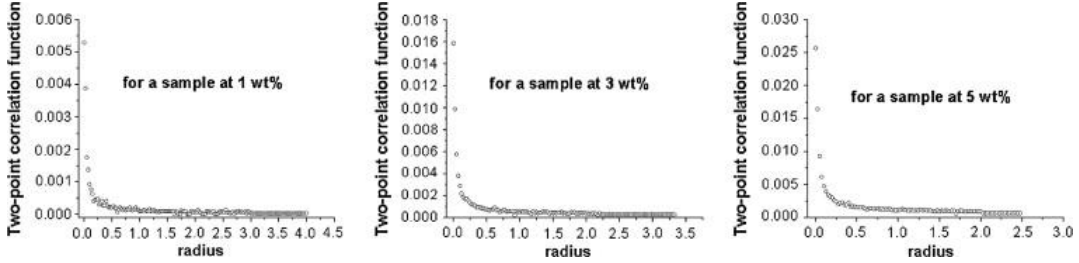


Figure 3.3. Results of 2-point correlation functions for composites at different weight fractions

Now that we already have the data of 1 and 2-point correlation functions, we can approximate the 3-point correlation function by the formula given in [9]:

$$S_3(x_1, x_2, x_3) \approx \left[ \frac{l_{x_1 x_2}}{l_{x_1 x_2} + l_{x_1 x_3}} S_2(x_1, x_3) \frac{l_{x_1 x_3}}{l_{x_1 x_2} + l_{x_1 x_3}} S_2(x_1, x_2) \right] \frac{S_2(x_2, x_3)}{S_1(x_1)} \quad (3.46)$$

With the aid of section 3.4, we are now able to determine the effective stiffness.

Recall (3.41):

$$\phi_p^2 L^{(q)} : [L_e^{(q)}]^{-1} = \phi_p I - \sum_{n=2}^{\infty} B_n^{(p)}$$

[3] showed that, for statistically isotropic materials, left hand side of (3.41) can be reduced to

$$\phi_p^2 \left[ \frac{\kappa_{pq}}{\kappa_{eq}} \Lambda_h + \frac{\mu_{pq}}{\mu_{eq}} \Lambda_s \right] = \phi_p I - \sum_{n=2}^{\infty} B_n^{(p)} \quad (3.47)$$

For simplicity, we take the first two terms in the infinite sum to represent the whole series.

Then (3.47) becomes

$$\phi_p^2 \left[ \frac{\kappa_{pq}}{\kappa_{eq}} \Lambda_h + \frac{\mu_{pq}}{\mu_{eq}} \Lambda_s \right] = \phi_p I - B_2^{(p)} - B_3^{(p)} \quad (3.48)$$

By (3.42) and (3.43),

$$B_2^{(p)} = \int_{\epsilon} U^{(q)}(x_1, x_2) [S_2^{(p)}(x_1, x_2) - \phi_p^2] dx_2,$$

$$B_3^{(p)} = (-1) \left( \frac{1}{\phi_p} \right) \int dx_2 \int U^{(q)}(x_1, x_2) : U^{(q)}(x_2, x_3) \Delta_3^{(p)}(x_1, x_2, x_3) dx_3$$

where

$$\Delta_3^{(p)} = \begin{vmatrix} S_2^{(p)}(x_1, x_2) & S_1^{(p)}(x_2) \\ S_3^{(p)}(x_1, x_2, x_3) & S_2^{(p)}(x_2, x_3) \end{vmatrix} \quad (3.49)$$

Now combine (3.48), (3.42), (3.43) and (3.49), one can plot figure 3.1 without any difficulties.

## Conclusions

We have investigated a statistical approach to report the effective stiffness of a 2-phase composite material by first exploiting the background knowledge as well as tools, then comparing the experimental results with the simulation results conducted after the strong-contrast series expansion with only the first two terms. It turns out to be an effective approach for 1% wt.% PA-OMMT composite, but fails when weight percentage increases. We suppose that the underlying reason is that we have no knowledge on the convergence rate of the series developed in last chapter. The series converge slowly for large wt.% because the n-point correlation function for large n then become nonnegligible due to the increased volume fraction of the minor phase. Substituting only the first two terms in (3.47) leads to a loss of information. On the other hand, although we can approximate 3-point correlation functions from 1, 2-correlation functions, we have yet no idea about how to compute higher order n-point correlation functions, say, 4-point correlation function, for the need of substituting more terms in (3.47). This is the point where further attention should be paid.

## Bibliography

- [1] Torquato S . Random Heterogeneous Materials[M]. Springer New York, 2002.
- [2]里斯, J.A , 田金方. 数理统计与数据分析(原书第 3 版)[M]. 机械工业出版社, 2011.
- [3] Torquato S . Effective stiffness tensor of composite media—I. Exact series expansion[J]. Journal of the Mechanics and Physics of Solids, 1997, 45(9):1421-1448.
- [4] Pham D C . Strong-contrast expansion correlation approximations for the effective elastic moduli of multiphase composites[J]. Archive of Applied Mechanics, 2012, 82(3):377-389.
- [5]常庚哲, 史济怀. 数学分析教程. 下册[M]. 高等教育出版社, 2003.
- [6] Y Rémond, Ahzi S , Baniassadi M , et al. Applied RVE Reconstruction and Homogenization of Heterogéneous Materials[M]. Wiley, 2016.
- [7] Baniassadi M , Laachachi A , Hassouna F , et al. Mechanical and thermal behavior of nanoclay based polymer nanocomposites using statistical homogenization approach[J]. Composites Science & Technology, 2011, 71(16):1930-1935.
- [8] Baniassadi M , Garmestani H , Li D S , et al. Three-phase solid oxide fuel cell anode microstructure realization using two-point correlation functions[J]. Acta Materialia, 2011, 59(1):30-43.
- [9] Mikdam A , Makradi A , Ahzi S , et al. A new approximation for the three-point probability function[J]. International Journal of Solids and Structures, 2009, 46:3782-3787.